Original Article

Artificial neural network approach for calculating mass attenuation coefficient of different glass systems

A. Benhadjira [a,*], M.I. Sayyed [b,c], O. Bentouila [a], K.E. Aiadi [a]

[a] Équipe Optoélectronique, LENREZA Laboratory, University of Kasdi Merbah, Ouargla, 30000, Algeria
[b] Department of Physics, Faculty of Science, Isra University, Amman, Jordan
[c] Department of Nuclear Medicine Research, Institute for Research and Medical Consultations (IRMC), Imam Abdulrahman bin Faisal University (IAU), P.O. Box 1982, Dammam 31441, Saudi Arabia

ARTICLE INFO

ABSTRACT

In this study, we propose an alternative approach using Artificial Neural Networks (ANN) for determining Mass Attenuation Coefficients (MAC) in various glass systems. This method takes into account the weights of glass compositions, density, and photon energy as input features. The ANN model was trained and tested on a dataset consisting of 650 data points and subsequently validated through a K-fold cross-validation procedure. Our findings demonstrate a high level of accuracy, with R^2 values ranging from 0.90 to 0.99. Additionally, the model exhibits robust extrapolation capabilities with an R^2 score of 0.87 for predicting MAC values in a new glass system. Furthermore, this approach significantly reduces the need for costly and time-consuming computations and experiments, making it a potential tool for selecting materials for effective radiation protection.

1. Introduction

Radiation in the environment that can cause ionization occurs constantly and can originate from either natural or man-made sources. Radiation can be emitted from both naturally occurring and artificial sources. Radionuclides in the atmosphere, water, rocks, and soil water are all examples of radiation that comes from natural sources. Natural radiation can also come from cosmic rays. nuclear accidents, nuclear power plants, nuclear weapon testing, research labs, and other sources can all manufacture synthetic radionuclides for various purposes [1–3]. Ionizing radiation is utilized—regularly in a wide variety of disciplines, including industry, energy, medical diagnostics, and other technological applications. Unfortunately, there is cause for concern regarding the potential adverse long-term repercussions of rising ionizing radiation exposure caused by growing usage [4–6]. In addition, a variety of investigations have shown that the annual number of people who pass away from cancer for reasons that might be strongly linked to radiation exposure is growing. When radiation is used frequently, it is necessary to take safety measures to protect human beings from being exposed to it. Ionizing radiation comes in a variety of forms, the most dangerous of which are X-rays and gamma rays (photons), which may pass through solid things and travel extremely long distances [7–10]. On the other hand, if one is exposed to photons for an extended period of time, they can cause cancer, genetic damage, the destruction of blood cells, and even death. As a result, it is essential to minimize exposure periods as low as possible by minimizing the amount of time spent near radiation sources and maintaining the maximum practical distance between individuals and radiation sources. One such law is known as the inverse square law, and it states that the intensity of radiation is proportional to the inverse of the square of the distance from the source [11–14].

Over the years, different materials have been used for radiation shielding applications, including ceramics, bricks, alloys, glasses, polymers, and nanocomposites for a variety of applications [15–17]. Understanding how gamma rays interact with matter is crucial in order to protect against them [18,19]. The mass attenuation coefficient (MAC) is a basic parameter that can describe the photon–matter interaction. So, it is important to determine the MAC for different materials in order to decide which material can be effectively used for protection from gamma radiation. There are different ways to determine the MAC such as using theoretical calculations with the help of known software (WinXom, Phy-X, etc.), experimental methods, and simulation approaches [20–23]. Experimental results are unsatisfactory for every energy range, and varied material kinds and the rapid expansion of materials made this work fruitless. Monte Carlo simulations are also employed in the process of finding MAC for particular types of materials; however, they can demand a significant amount of computational

* Corresponding author.
  E-mail addresses: benhadjira.abdelrahman@univ-ouargla.dz (A. Benhadjira), dr.mabualssayed@gmail.com (M.I. Sayyed).

time. When performing theoretical calculations, despite the fact that the basic principles are familiar, it is typically challenging to identify a precise solution to real-world physical problems [24–27].

Machine learning algorithms are currently being employed in every sector, from the field of particle physics [28] to material science [29, 30], and even solving inverse design problems [31,32], whenever it is necessary to analyze complicated data. They are particularly helpful in the field of non-linear regression, and in theory, they can model any curve. Artificial Neural Networks (ANNs), which are capable of recognizing difficult correlations and patterns across datasets, are emerging as a powerful tool that has grown increasingly popular in the field of machine learning. This popularity can be attributed to the fact that ANNs are able to comprehend complex patterns. By being trained on vast quantities of previously determined radiation shielding data, such as MAC values, ANNs are able to generalize their findings and produce accurate predictions for additional data. The utilization of ANNs in the prediction of the MAC for materials gives a number of important advantages that cannot be achieved by other standard methods. Artificial neural networks (ANNs) have the power to express advanced nonlinear relationships between the glasses' composition and their MAC, which may be difficult to model using standard mathematical methods. These interactions can be caused by the fact that the glasses are made up of several components. Furthermore, ANNs excel at automatically identifying the variables that have the greatest impact on the MAC by gathering useful traits from the input data. This reduces the need for human feature selection or prior knowledge of fundamental physics, allowing the model to show subtle correlations that human-designed methods could overlook. The ANN's ability to learn and adapt lets it notice complex information and nonlinear connections that facilitate precise MAC predictions. The ability of ANNs to manage datasets that are both extensive and diverse is an additional advantage of utilizing these models.

The primary objective of this research is to present confirmation that ANN models are helpful for precisely predicting the MAC of various glass systems. We seek to develop a reliable predictive model by instructing an artificial neural network (ANN) using a comprehensive list of glass compositions and the MAC values associated with each of those compositions. This will make it possible for us to determine the MAC for glasses in a way that is not only accurate but also time-effective. The ANN model that was suggested has the capability to significantly reduce the necessity for sophisticated computational computations or experimental observations. As a consequence of this, it has the potential to supply both academics and industry professionals with a useful tool for the rapid prediction of the MAC of various glasses.

2. Methodology

2.1. Data analysis

In this study, we aim to investigate the relationship between the molar fraction density and energy of oxide glasses containing the components PbO, WO_3, Li_2O, B_2O_3, GeO_2, BaO, MoO_3 and P_2O_5 and their mass attenuation coefficient. The data herein were collected from published scientific papers [33–36]. The dataset comprises 650 rows and 11 features, including glass composition molar fraction in (wt%), glass density, energy ranging from 0.015 to 15 MeV, and the target variable, mass attenuation coefficient in (cm^2/g). which is a function of the energy and the atomic number of the material [36] and can be calculated using the following equation:

$$MAC = \sum \omega_i (\frac{\mu}{\rho})_i \tag{1}$$

where ω_i and $(\frac{\mu}{\rho})_i$ are the weight fraction and the mass attenuation coefficient of ith element respectively, which can be obtained experimentally or collected from XCOM or WinXCom program [37]

Descriptive statistics were computed to summarize the dataset, and the results are presented in Table 1. The table includes the count, mean,

Table 1
Statistical summary of the dataset.

	count	mean	std	min	25%	50%	75%	max
PbO	650.00	12.12	19.98	0.00	0.00	0.00	20.00	60.00
Bi_2O_3	650.00	5.00	7.47	0.00	0.00	0.00	10.00	20.00
WO_3	650.00	1.92	3.94	0.00	0.00	0.00	0.00	10.00
Li_2O	650.00	8.85	11.72	0.00	0.00	2.50	10.00	40.00
B_2O_3	650.00	31.92	26.81	0.00	0.00	27.50	60.00	70.00
GeO_2	650.00	2.50	6.97	0.00	0.00	0.00	0.00	30.00
BaO	650.00	16.92	16.60	0.00	0.00	15.00	30.00	50.00
MoO_3	650.00	10.77	20.57	0.00	0.00	0.00	10.00	70.00
P_2O_5	650.00	10.00	16.30	0.00	0.00	0.00	20.00	50.00
Density (g/cm^3)	650.00	4.47	1.41	2.55	3.49	3.87	5.87	7.08
E (Mev)	650.00	2.35	3.72	0.01	0.08	0.50	3.00	15.00
MAC (cm^2/g)	650.00	4.74	13.95	0.02	0.04	0.10	1.94	99.79

standard deviation (std), minimum (min), and maximum (max) values, as well as the 25th, 50th, and 75th quartiles.

Additionally, the distribution of the mass attenuation coefficient (MAC) using Kernel Density Estimation (KDE) is illustrated in Fig. 1. The distribution appears to be skewed toward zero, resulting in a Gaussian distribution centered around zero. The majority of the values fall between zero and 20, while the remaining values are sparsely distributed between 20 and 90.

Furthermore, Fig. 2 shows the correlation matrix. Positive correlations are observed between MAC and PbO, Bi_2O_3, WO_3, GeO_2, and density, with corresponding p-values ranging from 0.15 to 0.19. These results suggest that higher concentrations of these oxides in a material may lead to an increase in its mass attenuation coefficient.

On the other hand, negative correlations are observed between MAC and Li_2O, B2O3, and BaO, with respect to energy. This indicates an inverse relationship between the concentrations of these oxides and MAC. However, it is important to note that the p-values are less than 1, indicating that there is no linear relationship between these variables and the mass attenuation coefficient.

2.2. Artificial neural networks

Artificial Neural Network (ANN) [38], also known as a multilayer perceptron (MLP), is a powerful machine learning model widely used in regression tasks due to its flexibility (universal approximation) [39]. It consists of multiple layers, including an input layer, hidden layers, and an output layer. Each layer is composed of individual neurons that perform mathematical computations, taking input variables and producing corresponding output values.

More formally, considering the output of the ith neuron in the jth hidden layer. Denoted as y_i is determined by the weights (w_i) associated with the neuron's connections and the input values (x_i). Additionally, a bias term (b_i) is added to the weighted sum of inputs:

$$y_i = w_i^T x_i + b_i \tag{2}$$

The output of the jth hidden layer, denoted as h_i, it can be expressed as a function (f) applied to the weighted sum of inputs ($\sum_{i=1}^{n} \omega_i x_i + b_i$). The activation function f is typically a non-linear function, allowing the neural network to capture complex relationships between inputs and outputs:

$$h_j = f \left(\sum_{i=1}^{n} \omega_i x_i + b_i \right) \tag{3}$$

Three types of activation functions were used in this work Exponential Linear Unit (ELU), Rectified Linear Unit (ReLU), and Sigmoid

$$ELU(x, \alpha) = \begin{cases} x & \text{if } x > 0 \\ \alpha \cdot (e^x - 1) & \text{if } x \leq 0 \end{cases} \tag{4}$$

$$ReLU(x) = \max(0, x) \tag{5}$$
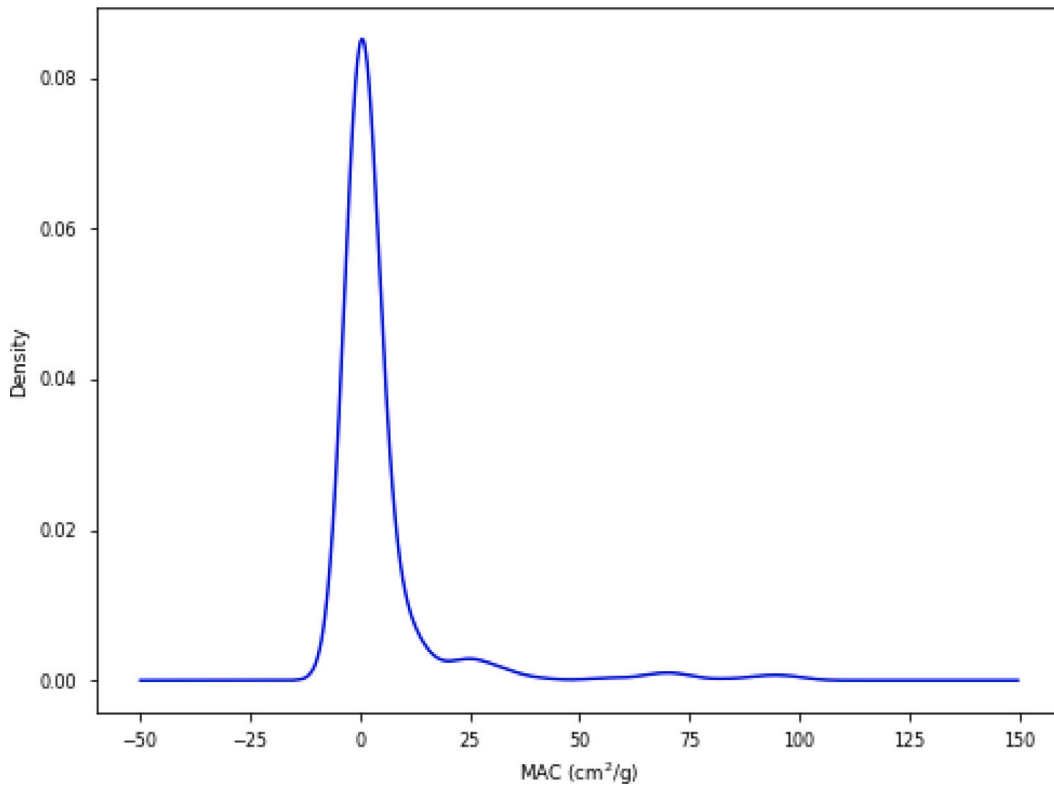
Fig. 1. Dataset mass attenuation coefficient distribution.
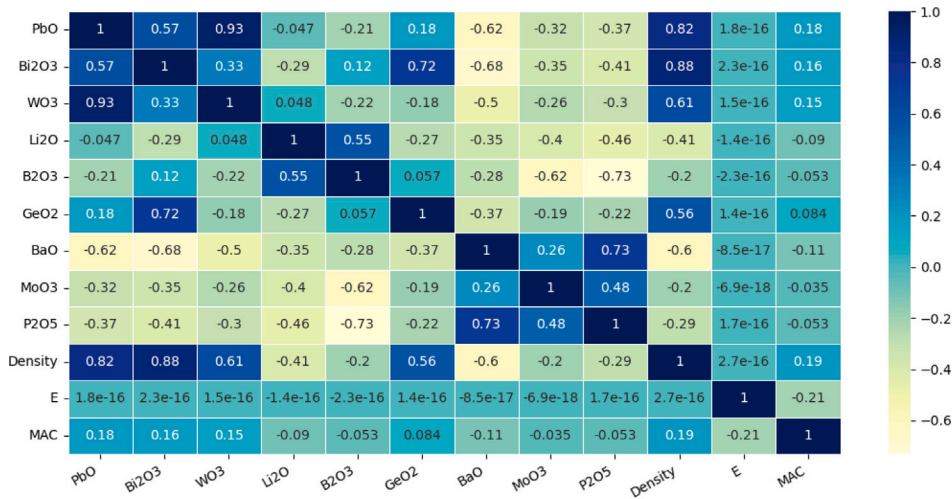
Fig. 2. Pearson correlation coefficient matrices heatmap.

$$Sigmoid(x) = \frac{1}{1 + e^{-x}} \qquad (6)$$

During the training process of an ANN, the back-propagation learning algorithm is employed [40]. This algorithm aims to adjust the network weights based on the calculated error (Loss) between the predicted outputs and the actual values of MAC, iteratively updating the weights to minimize this error.

To optimize the learning process, a gradient descent optimizer called ADAM (Adaptive Moment Estimation) is used [41] to improve the training performance. ADAM adapts the learning rate for each weight parameter based on both the gradient descent and the previous updates. More details about our ANN including the number of nodes in each layer, activation functions, dropout rates, number of epochs (iterations), and the learning rate. are provided in Table 2

2.3. Evaluation method

The performance of the artificial neural network was evaluated using k-fold cross-validation. The dataset is divided into k equally sized folds and the model is then trained and tested k time, each time $(k-1)$ of the folds as a training set and the remaining fold for testing the model.

To quantify the fitness and accuracy of the models, the coefficient of determination (R^2) and root mean squared error (RMSE) were employed as evaluation metrics. These metrics are defined as follows:

$$R^2 = 1 - \frac{\sum_{i=1}^{n}(y'i - y_i)^2}{\sum i = 1^n (y_i - \hat{y})^2} \qquad (7)$$

Table 2
Artificial neural network specifications.

Layer	Number of nodes	Activation function	Dropout rate
Input layer	7	Linear	non
1st hidden layer	110	Elu (Exponential Linear Unit)	0.15
2nd hidden layer	90	Sigmoid	0.10
3rd hidden layer	30	ReLU (Rectified Linear Activation Function)	non
Output layer	1 (Mac)	Linear	non
Number of Epochs	5000		
Learning Rate	0.001		
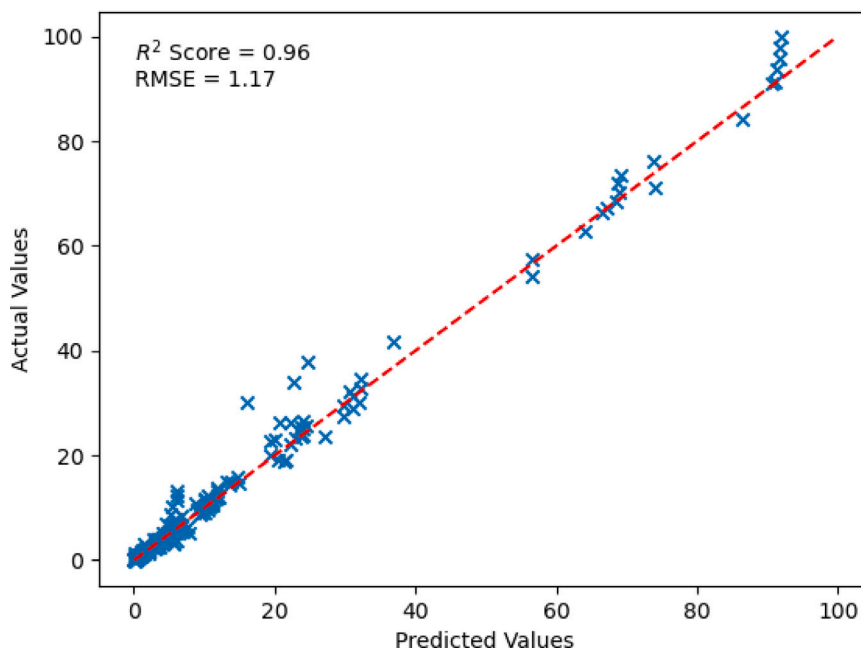
Fig. 3. Predicted versus the actual values of the mass attenuation coefficient.

$$RMSE = \sqrt{\frac{1}{N}\sum_{i=1}^{N}(y_i' - y_i)^2} \qquad (8)$$

Here, N represents the total number of samples, y_i' denotes the model-predicted value, y_i represents the actual value, and $\hat{y}$ is the average of the actual values. The coefficient of determination, R^2, is a non-negative metric ranging from 0 to 1. It measures the model's robustness in fitting the real data, with a value closer to 1 indicating a better-fitting model. On the other hand, the accuracy of the model is considered good when the RMSE tends to 0, indicating that the predicted values are close to the actual values.

3. Result and discussion

Calculating the mass attenuation coefficient of materials is vital for nuclear science, as a result, we have established an artificial neural network to predict the MAC of different glasses as recapitulated in Table 2. We have noticed that the data is sparse (many zeros), hence, we have used the L1 norm as a loss function (the sum of the absolute values). This loss function is particularly useful when dealing with sparse data. Additionally, the L1 norm is less sensitive to outliers compared to other loss functions [42]. To reduce overfitting we have included a dropout regularization rate during the training phase [43]. The proposed ANN was implemented using the Pytorch framework which is an artificial intelligence Python library.

After constructing the artificial neural networks we split the data into 5 folds for cross-validation, the ANN was repeatedly trained with 4 folds and tested for the remaining fold. The results are shown in the Table 3 and visually summarized in Fig. 3. The results indicate a high level of model performance with a R^2 score ranging from 0.90 to 0.99 and an average of 0.95. The RMSE of the testing folds are relatively low ranging from 0.67 to 2.11, with an average of 1.91. However, we can observe that the model deviate in predicting certain point of the data as shown in Fig. 3 this is because of the skewness of the MAC distribution as shown in Fig. 1 and discussed in the data analysis section, in this context these points are considered to be outliers as the MAC values are highly populated between 0 and 40 which results in a heavy tail compared to the other values

To assess the capability of generalization of our model, we conducted predictions for the mass attenuation coefficient (MAC) of additional glass samples (see Table 4) that were not included in the cross-validation procedure. In Fig. 4 we present a visual representation of the actual MAC values versus the predicted values for these corresponding glasses.

Remarkably, the model demonstrates impressive accuracy in predicting 100 MAC values, achieving a high R^2 score of 0.89. This indicates that the model can accurately predict a substantial portion of the data, showcasing its strong predictive capabilities. However, it is essential to note that the relatively high root mean square error (RMSE) of 5.58 suggests that there are still some variations between the predicted and actual values.

Overall, the results indicate that the model shows promising predictive and generalization ability, as evidenced by its accurate predictions for both the cross-validation phase and the additional glass samples MAC prediction. The high R^2 score further validates the model's proficiency in capturing the underlying relationships between the input
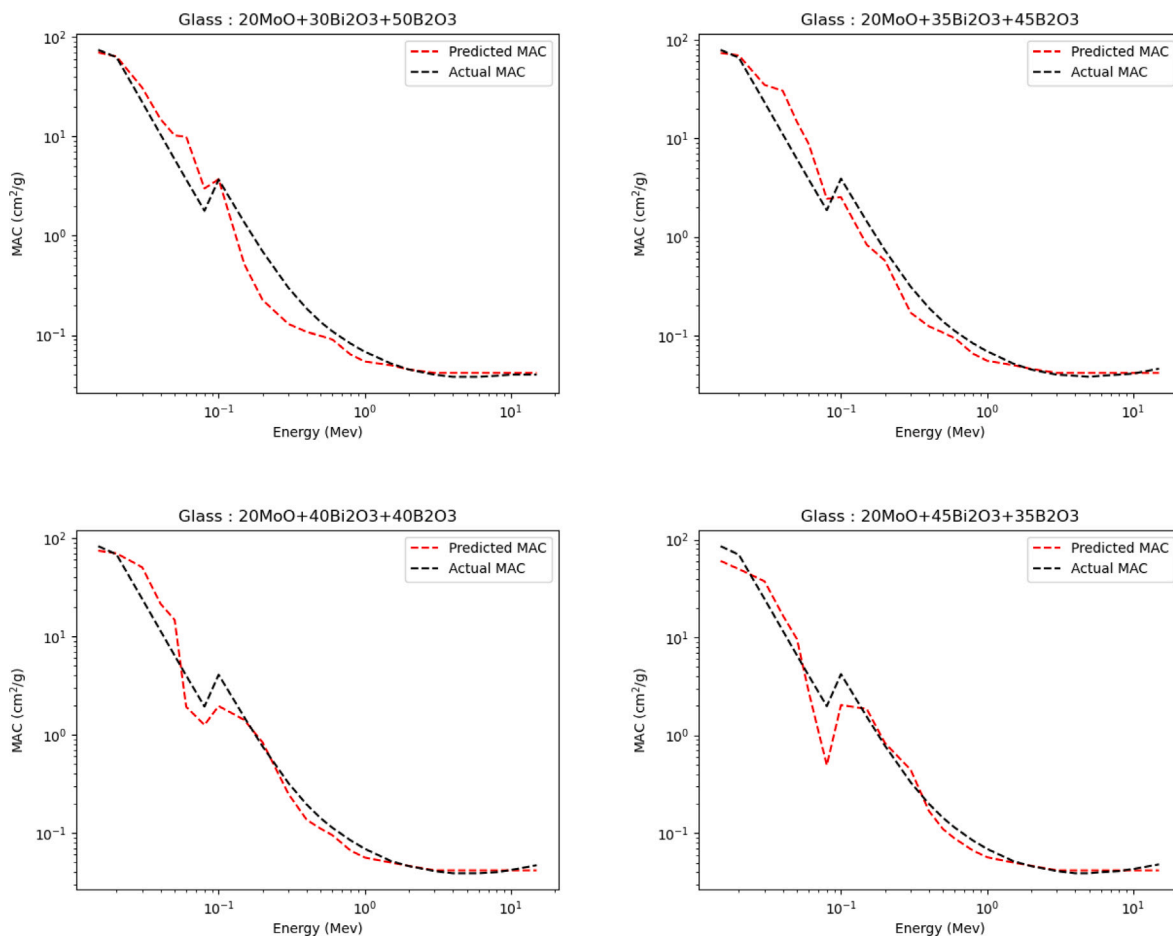
Fig. 4. Comparison of predicted and actual mass attenuation coefficients for new glasses.

Table 3
R2 score and RMSE of the cross-validation folds.

Fold	R2 score	RMSE
Fold 1	0.99	1.18
Fold 2	0.99	0.67
Fold 3	0.90	2.11
Fold 4	0.98	0.67
Fold 5	0.95	1.23
Mean	**0.96**	**1.17**

Table 4
The densities (g/cm^3) and chemical compositions (mol%) of $MoO_3 - Bi_2O_3 - B_2O_3$ glass system for validation.

Sample	MoO_3 (%)	Bi_2O_3 (%)	B_2O_3 (%)	Density
S1	20	30	50	4.807
S2	20	35	45	5.151
S3	20	40	40	5.559
S4	20	45	35	5.807

features and the MAC values, making it a reliable tool for mass attenuation coefficient predictions in diverse glass compositions. Nevertheless, further analysis and improvements with more data and including other physical properties could be considered to reduce the RMSE and enhance the model's overall performance.

4. Conclusion

In conclusion, a dataset comprising 650 glass mass attenuation coefficients was employed to construct an artificial neural network for the calculation of MAC values of glasses. The data underwent a k-fold cross-validation process to assess the model's performance, yielding R^2 scores ranging from 0.90 to 0.99 for the testing folds. Moreover, to verify the model's generalization capability, our model was tested on 100 MAC values of new glasses, achieving excellent prediction performance with an R^2 score of 0.87. Which demonstrates the reliability of artificial neural networks as a tool for MAC calculation.

Incorporating ANN into the estimation of the MAC of different glass systems has indeed unveiled new avenues for fast and effective glass evaluation. The predictive abilities of ANN position it as an essential tool for future radiation shielding studies. Furthermore, there is still more work to be done in this domain, such as exploring other machine learning techniques, gathering additional data, and incorporating other covariates to enhance prediction performance. By continually advancing in these areas, researchers can further improve their understanding of the radiation shielding properties of materials.

Declaration of competing interest

The authors declare that they have no known competing financial interests or personal relationships that could have appeared to influence the work reported in this paper.

References

[1] M. Kamislioglu, An investigation into gamma radiation shielding parameters of the (Al: Si) and (Al+ Na): Si-doped international simple glasses (ISG) used in nuclear waste management, deploying Phy-X/PSD and SRIM software, J. Mater. Sci., Mater. Electron. 32 (2021) 12690–12704.

[2] Ran Li, Yizhuo Gu, Gaolong Zhang, Zhongjia Yang, Min Li, Zuoguang Zhang, Radiation shielding property of structural polymer composite: Continuous basalt fiber reinforced epoxy matrix composite containing erbium oxide, Compos. Sci. Technol. 143 (2017) 67–74.

[3] Nazlıcan Şahin, Merve Bozkurt, Yaşar Karabul, Mehmet Kılıç, Zeynep Güven Özdemir, Low cost radiation shielding material for low energy radiation applications: Epoxy/Yahyali Stone composites, Prog. Nucl. Energy 135 (2021) 103703.

[4] Turgay Korkut, Zeynep Itır Umaç, Bünyamin Aygün, Abdulhalik Karabulut, Sinan Yapıcı, Remzi Şahin, Neutron equivalent dose rate measurements of gypsum-waste tire rubber layered structures, Int. J. Polymer Anal. Charact. 18 (6) (2013) 423–429.

[5] M. Kamislioglu, Research on the effects of bismuth borate glass system on nuclear radiation shielding parameters, Results Phys. 22 (2021) 103844.

[6] Rishu Prasad, Avinash R. Pai, S. Olutunde Oyadiji, Sabu Thomas, S.K.S. Parashar, Utilization of hazardous red mud in silicone rubber/MWCNT nanocomposites for high performance electromagnetic interference shielding, J. Clean. Prod. 377 (2022) 134290.

[7] Tonguç Özdemir, Seda Nur Yılmaz, Mixed radiation shielding via 3-layered polydimethylsiloxane rubber composite containing hexagonal boron nitride, boron (III) oxide, bismuth (III) oxide for each layer, Radiat. Phys. Chem. 152 (2018) 17–22.

[8] T. Özdemir, A. Güngör, I.K. Akbay, H. Uzun, Y. Babuçcuoglu, Nano lead oxide and epdm composite for development of polymer based radiation shielding material: Gamma irradiation and attenuation tests, Radiat. Phys. Chem. 144 (2018) 248–255.

[9] Amandeep Sharma, M.I. Sayyed, O. Agar, H.O. Tekin, Simulation of shielding parameters for TeO2-WO3-GeO2 glasses using FLUKA code, Results Phys. 13 (2019) 102199.

[10] Shams A.M. Issa, Ashok Kumar, M.I. Sayyed, M.G. Dong, Y. Elmahroug, Mechanical and gamma-ray shielding properties of TeO2-ZnO-NiO glasses, Mater. Chem. Phys. 212 (2018) 12–20.

[11] Seulgi Kim, Yunhee Ahn, Sung Ho Song, Dongju Lee, Tungsten nanoparticle anchoring on boron nitride nanosheet-based polymer nanocomposites for complex radiation shielding, Compos. Sci. Technol. 221 (2022) 109353.

[12] S. Yonphan, W. Chaiphaksa, E. Kalkornsurapranee, A. Tuljittraporn, S. Kothan, S. Kaewjaeng, N. Intachai, N. Wongdamnern, C. Kedkaew, H.J. Kim, et al., Development of flexible radiation shielding materials from natural rubber/Sb2o3 composites, Radiat. Phys. Chem. 200 (2022) 110379.

[13] Mengge Dong, Xiangxin Xue, He Yang, Zhefu Li, Highly cost-effective shielding composite made from vanadium slag and boron-rich slag and its properties, Radiat. Phys. Chem. 141 (2017) 239–244.

[14] Mengge Dong, Xiangxin Xue, He Yang, Dong Liu, Chao Wang, Zhefu Li, A novel comprehensive utilization of vanadium slag: As gamma ray shielding material, J. Hazard. Mater. 318 (2016) 751–757.

[15] Dalal A. Aloraini, M.Y. Hanfi, M.I. Sayyed, K.A. Naseer, Aljawhara H. Almuqrin, P. Tamayo, O.L. Tashlykov, K.A. Mahmoud, Design and Gamma-ray attenuation features of new concrete materials for low- and moderate-photons energy protection applications, Materials 15 (14) (2022) 4947.

[16] Mayeen Uddin Khandaker, D.A. Bradley, Hamid Osman, M.I. Sayyed, A. Sulieman, M.R.I. Faruque, K.A. Naseer, Abubakr M. Idris, The significance of nuclear data in the production of radionuclides for theranostic/therapeutic applications, Radiat. Phys. Chem. 200 (2022) 110342.

[17] S.A. Bassam, K.A. Naseer, Anagha J. Prakash, K.A. Mahmoud, C.S. Suchand-Sangeeth, M.I. Sayyed, Mohammed S. Alqahtani, E. El Sheikh, Mayeen Uddin Khandaker, Effect of tm2o3 addition on the physical, structural, elastic, and radiation-resisting attributes of tellurite-based glasses, Radiat. Phys. Chem. 209 (2023) 110988.

[18] M.R. Ambika, N. Nagaiah, V. Harish, N.K. Lokanath, M.A. Sridhar, N.M. Renukappa, S.K. Suman, Preparation and characterisation of isophthalic-Bi2O3 polymer composite gamma radiation shields, Radiat. Phys. Chem. 130 (2017) 351–358.

[19] Bünyamin Aygün, High alloyed new stainless steel shielding material for gamma and fast neutron radiation, Nucl. Eng. Technol. 52 (3) (2020) 647–653.

[20] Bünyamin Aygün, Neutron and gamma radiation shielding Ni based new type super alloys development and production by Monte Carlo simulation technique, Radiat. Phys. Chem. 188 (2021) 109630.

[21] Tianyu Zhang, Yang Li, Yan Yuan, Kai Cui, Wenjing Wei, Jinzhu Wu, Wei Qin, Xiaohong Wu, Spatially confined Bi2O3–Ti3C2Tx hybrids reinforced epoxy composites for gamma radiation shielding, Compos. Commun. 34 (2022) 101252.

[22] M.I. Sayyed, Ashok Kumar, H.O. Tekin, Ramandeep Kaur, Mandeep Singh, O. Agar, Mayeen Uddin Khandaker, Evaluation of gamma-ray and neutron shielding features of heavy metals doped Bi2O3-BaO-Na2O-MgO-B2O3 glass systems, Prog. Nucl. Energy 118 (2020) 103118.

[23] Fouad Ismail El-Agawany, Karem Abdel-Azeem Mahmoud, Hakan Akyildirim, El-Sayed Yousef, Huseyin Ozan Tekin, Yasser Saad Rammah, Physical, neutron, and gamma-rays shielding parameters for Na2O–SiO2–PbO glasses, Emerg. Mater. Res. 10 (2) (2021) 227–237.

[24] K.A. Mahmoud, F.I. El-Agwany, Y.S. Rammah, O.L. Tashlykov, Gamma ray shielding capacity and build up factors of CdO doped lithium borate glasses: theoretical and simulation study, J. Non-Crystalline Solids 541 (2020) 120110.

[25] W. Cheewasukhanont, P. Limkitjaroenporn, S. Kothan, C. Kedkaew, J. Kaewkhao, The effect of particle size on radiation shielding properties for bismuth borosilicate glass, Radiat. Phys. Chem. 172 (2020) 108791.

[26] S.A. Tijani, Yas Al-Hadeethi, Isa Sambo, F.A. Balogun, Shielding of beta and bremsstrahlung radiation with transparent Bi2O3-B2O3-TeO2 glasses in therapeutic nuclear medicine, J. Radiol. Prot. 38 (3) (2018) N44.

[27] Sevim Bilici, Mirac Kamislioglu, Elif Ebru Altunsoy Guclu, A Monte Carlo simulation study on the evaluation of radiation protection properties of spectacle lens materials, Eur. Phys. J. Plus 138 (1) (2023) 80.

[28] Kim Albertsson, et al., Machine learning in high energy physics community white paper, J. Phys. Conf. Ser. 1085 (2018) 022008.

[29] Abderrahmane Benhadjira, Omar Bentouila, Kamal Eddine Aiadi, Mohammed Adem Bourenane, Judd–Ofelt parameters prediction of Er+3 and Nd+3 doped oxide glasses using machine learning models, Optik 285 (2023) 170946.

[30] Daniel R. Cassar, GlassNet: a multitask deep neural network for predicting many glass properties, 2023, arXiv preprint arXiv:2303.15538.

[31] Qi Wang, Longfei Zhang, Inverse design of glass structure with deep graph neural networks, Nature Commun. 12 (2021).

[32] Dongping Chang, Wencong Lu, Gang Wang, Designing bulk metallic glasses materials with higher reduced glass transition temperature via machine learning, Chemometr. Intell. Lab. Syst. 228 (2022) 104621.

[33] Ashok Kumar, Anisha Jain, M.I. Sayyed, Farah Laariedh, K.A. Mahmoud, Jamel Nebhen, Mayeen Uddin Khandaker, M.R.I. Faruque, Tailoring bismuth borate glasses by incorporating PbO/GeO2 for protection against nuclear radiation, Sci. Rep. 11 (1) (2021).

[34] Atif Mossad Ali, M.I. Sayyed, Ashok Kumar, M. Rashad, Ali M. Alshehri, Ramandeep Kaur, Optically transparent newly developed glass materials for gamma ray shielding applications, J. Non-Crystalline Solids 521 (2019) 119490.

[35] Y. Al-Hadeethi, M.I. Sayyed, BaO–Li2O–B2O3 glass systems: Potential utilization in gamma radiation protection, Prog. Nucl. Energy 129 (2020) 103511.

[36] O. Agar, M.I. Sayyed, H.O. Tekin, Kawa M. Kaky, S.O. Baki, I. Kityk, An investigation on shielding properties of BaO, MoO3 and P2O5 based glasses using MCNPX code, Results Phys. 12 (2019) 629–634.

[37] L. Gerward, N. Guilbert, K.B. Jensen, H. Levring, WinXCom—a program for calculating X-ray attenuation coefficients, Radiat. Phys. Chem. 71 (3–4) (2004) 653–654.

[38] Ian Goodfellow, Yoshua Bengio, Aaron Courville, Deep Learning, MIT Press, 2016, http://www.deeplearningbook.org.

[39] Kurt Hornik, Maxwell Stinchcombe, Halbert White, Multilayer feedforward networks are universal approximators, Neural Netw. 2 (5) (1989) 359–366.

[40] Raúl Rojas, The backpropagation algorithm, in: Neural Networks: A Systematic Introduction, Springer Berlin Heidelberg, Berlin, Heidelberg, 1996, pp. 149–182.

[41] Diederik Kingma, Jimmy Ba, Adam: A method for stochastic optimization, Int. Conf. Learn. Represent. (2014).

[42] Qifa Ke, Takeo Kanade, Robust L1 norm factorization in the presence of outliers and missing data by alternative convex programming, in: Proceedings / CVPR, IEEE Computer Society Conference on Computer Vision and Pattern Recognition. IEEE Computer Society Conference on Computer Vision and Pattern Recognition, Vol. 1, 2005, pp. 739 – 746.

[43] Nitish Srivastava, Geoffrey Hinton, Alex Krizhevsky, Ilya Sutskever, Ruslan Salakhutdinov, Dropout: A simple way to prevent neural networks from overfitting, J. Mach. Learn. Res. 15 (56) (2014) 1929–1958.